

# STIFFNESS NONLINEARITY OF THREE SANDS

Authors

By Satoshi Yamashita,<sup>1</sup> Michele Jamiolkowski,<sup>2</sup> and Diego C. F. Lo Presti<sup>3</sup>

## Content

**ABSTRACT:** This paper presents the results of 254 drained triaxial compression tests. The results are analyzed with the aim of obtaining a phenomenological description of secant Young's modulus variation according to different test conditions. Using empirical fitting equations, the influences of different factors such as axial strain, vertical consolidation stress, consolidation stress ratio, and stress history on the secant Young's modulus under axisymmetric (triaxial) loading conditions at small and intermediate axial strains are singled out and presented. The main purpose of this paper is to identify the factors affecting the nonlinear secant stiffness of sand and to quantify their relevance at different levels of strain.

## Headline

### INTRODUCTION

Stiffness reduction with increasing strain and shear stress levels has been widely recognized in geotechnical engineering for the last half century. Moreover, more recently [e.g., Tatsuoka (1988)] the improvement achieved in the reliable measurement of soil behavior at small ( $\epsilon \cong 10^{-5}$ ) and intermediate strains ( $10^{-5} < \epsilon \leq 5 \times 10^{-3}$ ) in the laboratory has highlighted the degree of nonlinearity exhibited by soil stiffness, emphasizing the paramount importance of this phenomenon for predicting the displacement of geotechnical constructions.

Based on the above, this paper is aimed at the purely phenomenological description of the secant Young's modulus ( $E_{sec}$ ) nonlinearity at small and intermediate strains, as inferred from a large number of drained triaxial compression tests performed on three sands.

All the triaxial tests were performed on specimens prepared by means of an air pluvial deposition subjected thereafter to both isotropic and anisotropic consolidation. Both the local axial strain and the local radial strain were measured in many tests. The results obtained have been analyzed with the aim of quantifying the relevance of the different factors that influence the  $E_{sec}$  nonlinearity at small and intermediate strains of the three test sands.

### EXPERIMENTAL DATA

#### Test Sands

The soils used were Toyoura, Quiou, and Ticino sands. Toyoura sand has been widely used for laboratory stress-strain tests in Japan. Ticino sand has been used for Calibration Chamber and laboratory stress-strain tests in Italy since 1976. More recently, Quiou sand (a French sand) has also been used in Italian Calibration Chamber and stress-strain laboratory tests. Toyoura sand is a subangular, uniform, fine quartz sand that does not contain fines. Quiou sand is a subangular, well-graded, coarse to medium carbonate sand containing about 2% of fines. Quiou sand is a crushable material containing 73% in weight of shell fragments (Fioravante et al. 1994b). Ticino sand is a medium to coarse, uniform, predominantly silica sand that does not contain fines (Bellotti et al. 1996). The main physical properties of these sands are shown in Table 1.

#### Institutions and Publishers

<sup>1</sup>Assoc. Prof., Dept. of Civ. Engrg., Kitami Inst. of Technol., Koencho 165, Kitami 090-8507, Japan. E-mail: yamast@king.cc.kitami-it.ac.jp

<sup>2</sup>Prof., Dept. of Struct. and Geotech. Engrg., Tech. Univ. of Turin, Corso Duca degli Abruzzi 24, 10129 Torino, Italy.

<sup>3</sup>Prof., Dept. of Struct. and Geotech. Engrg., Tech. Univ. of Turin, Corso Duca degli Abruzzi 24, 10129, Torino, Italy. E-mail: diego.lopresti@polito.it

Note. Discussion open until March 2001. To extend the closing date one month, a written request must be filed with the ASCE Manager of Journals. The manuscript for this technical note was submitted for review and possible publication on February 18, 1999. This technical note is part of the *Journal of Geotechnical and Geoenvironmental Engineering*, Vol. 126, No. 10, October, 2000. ©ASCE, ISSN 1090-0241/00/0010-0929-0938/\$8.00 + \$.50 per page. Technical Note No. 20285.

header/footer

JOURNAL OF GEOTECHNICAL AND GEOENVIRONMENTAL ENGINEERING / OCTOBER 2000 / 929

header/footer

J. Geotech. Geoenviron. Eng., 2000, 126(10): 929-938

## Headline

### Sample Preparation

Specimens with 70 mm in diameter and 140 mm in height were reconstituted by dry pluvial deposition method. Only for some tests on Ticino sand were smaller samples tested (i.e., 40 and 60 mm in diameter). The ratio of height to diameter  $H/D$  of all specimens is two.

Toyourea sand specimens were reconstituted to a void ratio after consolidation  $e_c$  ranging from 0.65 to 0.89 (i.e.,  $D_r = 25$  to 90%). For Quiou sand specimens, the  $e_c$  ranged between 0.79 and 1.04 (i.e.,  $D_r = 55$  to 105%), while for Ticino sand specimens the  $e_c$  ranged between 0.58 and 0.88 (i.e.,  $D_r = 15$  to 100%).

All the relevant information concerning the triaxial tests performed is given in Table 2.

## Headline

### Triaxial Tests

## Headline

#### Apparatus

The triaxial testing systems used for the tests, developed at ISMES (Istituto Sperimentale Modelli e Strutture, Italy) and the Technical University of Turin, are computer-controlled triaxial cells with internal tie rods. A load cell to measure the axial load without any piston friction is located inside the pressure chamber. In the triaxial apparatus developed at the Technical University of Turin, the loading ram is virtually frictionless. The axial strain was measured locally using high resolution submersible LVDTs, and externally. The details of the test apparatuses were described by Fioravante et al. (1994b), Jamiolkowski et al. (1994b), and Lo Presti et al. (1994).

Twenty-six tests on Toyoura sand and eight tests on Quiou sand were performed at the Technical University of Turin, while all the tests on the Ticino sand (184) and other tests on the Quiou sand (36) were performed at ISMES (Table 2). The axial strain was only measured externally for the majority of the Ticino sand tests.

## Headline

### Test Procedures

Two sets of drained triaxial compression tests were performed at constant axial strain rate and lateral pressure with confining stress ranging between 50 and 800 kPa. The first set

TABLE 1. Physical Properties of Tested Sands

figure Sand name	figure $G_s$	figure $D_{50}$ (mm)	figure Small (4)	figure Percentage fines ( $\leq 75 \mu m$ ) (5)	figure Small (6)	figure Small (7)
(1)	(2)	(3)	(4)	(5)	(6)	(7)
Toyourea sand	2.630	0.16	1.3	0	0.985	0.611
Quiou sand	2.710	0.41	4.5	0	0.988	0.831
Ticino sand	2.690	0.55	1.6	0	0.934	0.582

Downloaded from ascelibrary.org by Massachusetts Institute of Technology (MIT) on 05/23/23. Copyright ASCE. For personal use only; all rights reserved.

TABLE 2. List of Test Conditions

figure Sand name (1)	figure Consolidation (2)	figure OCR (3)	figure small figure (kPa) (4)	figure small figure (5)	figure D (mm) (6)	figure small figure (mm) (7)	figure Number of tests (8)	figure Laboratory (9)
figure Toyoura sand	figure Isotropic consolidation	figure small figure 100	figure small figure 50–140	figure small figure 0.648–0.886	figure small figure 70	figure small figure 140	figure small figure 14	figure small figure Turin
	figure $K_0$ consolidation	figure small figure 100–180	figure small figure 100	figure small figure 0.59–0.885	figure small figure 70	figure small figure 140	figure small figure 4	figure small figure Turin
figure Quiou sand	figure Isotropic consolidation	figure small figure 50–100	figure small figure 40–100	figure small figure 0.92–1.024	figure small figure 70	figure small figure 140	figure small figure 24	figure small figure ISMES
		figure small figure 100	figure small figure 100	figure small figure 0.852–0.948	figure small figure 70	figure small figure 140	figure small figure 2	figure small figure ISMES
		figure small figure 100	figure small figure 100	figure small figure 0.865–1.000	figure small figure 70	figure small figure 140	figure small figure 2	figure small figure ISMES
		figure small figure 100	figure small figure 100	figure small figure 1.001	figure small figure 70	figure small figure 140	figure small figure 2	figure small figure ISMES
	figure $K_0$ consolidation	figure small figure 100–500	figure small figure 100	figure small figure 0.810–0.896	figure small figure 70	figure small figure 140	figure small figure 2	figure small figure ISMES
		figure small figure 100–500	figure small figure 100	figure small figure 0.724–1.036	figure small figure 70	figure small figure 140	figure small figure 2	figure small figure ISMES
		figure small figure 100–500	figure small figure 100	figure small figure 0.932–0.979	figure small figure 70	figure small figure 140	figure small figure 2	figure small figure ISMES
		figure small figure 100–500	figure small figure 100	figure small figure 0.879–1.003	figure small figure 70	figure small figure 140	figure small figure 2	figure small figure ISMES
figure Ticino sand	figure Isotropic consolidation	figure small figure 50–800	figure small figure 50–800	figure small figure 0.596–0.816	figure small figure 60–70	figure small figure 120–140	figure small figure 39	figure small figure ISMES
		figure small figure 50–800	figure small figure 50–800	figure small figure 0.600–0.708	figure small figure 60–70	figure small figure 120–140	figure small figure 39	figure small figure ISMES
		figure small figure 50–800	figure small figure 50–800	figure small figure 0.602–0.783	figure small figure 60–70	figure small figure 120–140	figure small figure 39	figure small figure ISMES
		figure small figure 50–800	figure small figure 50–800	figure small figure 0.654–0.714	figure small figure 60–70	figure small figure 120–140	figure small figure 39	figure small figure ISMES
		figure small figure 50–800	figure small figure 50–800	figure small figure 0.602–0.758	figure small figure 60–70	figure small figure 120–140	figure small figure 39	figure small figure ISMES
	figure $K_0$ consolidation	figure small figure 150–1,450	figure small figure 150–1,450	figure small figure 0.577–0.814	figure small figure 40–70	figure small figure 80–140	figure small figure 32	figure small figure ISMES
		figure small figure 150–1,450	figure small figure 150–1,450	figure small figure 0.615–0.782	figure small figure 40–70	figure small figure 80–140	figure small figure 32	figure small figure ISMES
		figure small figure 150–1,450	figure small figure 150–1,450	figure small figure 0.608–0.773	figure small figure 40–70	figure small figure 80–140	figure small figure 32	figure small figure ISMES
		figure small figure 150–1,450	figure small figure 150–1,450	figure small figure 0.616–0.795	figure small figure 40–70	figure small figure 80–140	figure small figure 32	figure small figure ISMES
		figure small figure 150–1,450	figure small figure 150–1,450	figure small figure 0.608–0.881	figure small figure 40–70	figure small figure 80–140	figure small figure 32	figure small figure ISMES
		figure small figure 150–1,450	figure small figure 150–1,450	figure small figure 0.595–0.776	figure small figure 40–70	figure small figure 80–140	figure small figure 32	figure small figure ISMES
		figure small figure 150–1,450	figure small figure 150–1,450	figure small figure 0.596–0.785	figure small figure 40–70	figure small figure 80–140	figure small figure 32	figure small figure ISMES

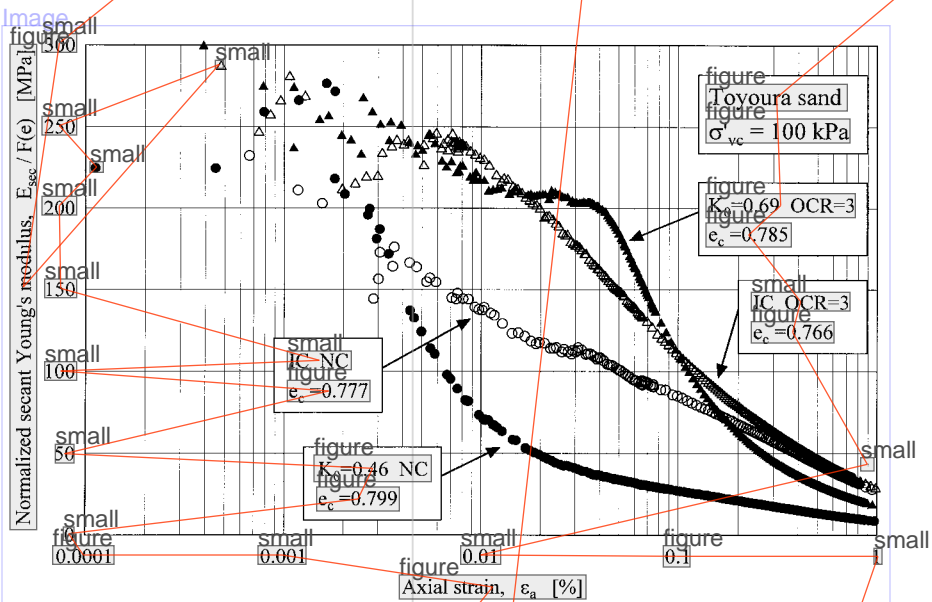


FIG. 1. Secant Young's Modulus versus Axial Strain of Toyoura Sand

was performed on isotropic normally consolidated (NC) and overconsolidated (OC) specimens. The second set was performed on  $K_0$  (the condition of zero radial strain) NC and OC specimens. The  $K_0$  condition was obtained by adjusting the cell pressure as the axial stress increased in order to prevent radial displacement. The radial deformation was measured locally using two proximity transducers placed horizontally on the specimen. The adopted overconsolidation ratio ( $OCR = \sigma'_{vm}/\sigma'_v$ ) ranged between 1.2 and 8. After the consolidation stage, a rest period of 1 to 2 h was adopted before starting the shearing phase.

The shearing stage of triaxial tests was carried out in drained conditions, under a strain-controlled frame, at a constant rate

of axial strain (about 0.01%/min). The radial pressure was kept constant.

The consolidation stress ratio, OCR, and effective vertical stress at the end of consolidation are also shown in Table 2.

Typical results of the triaxial compression tests on Toyoura and Quiou sands are shown in Figs. 1 and 2. These figures show the secant Young's modulus  $E_{sec}$  versus the axial strain, plotted in logarithmic scale, for four compression loading tests with almost the same void ratio (Toyourea sand: 0.77–0.80; Quiou sand: 0.87–0.89) and the effective vertical consolida-

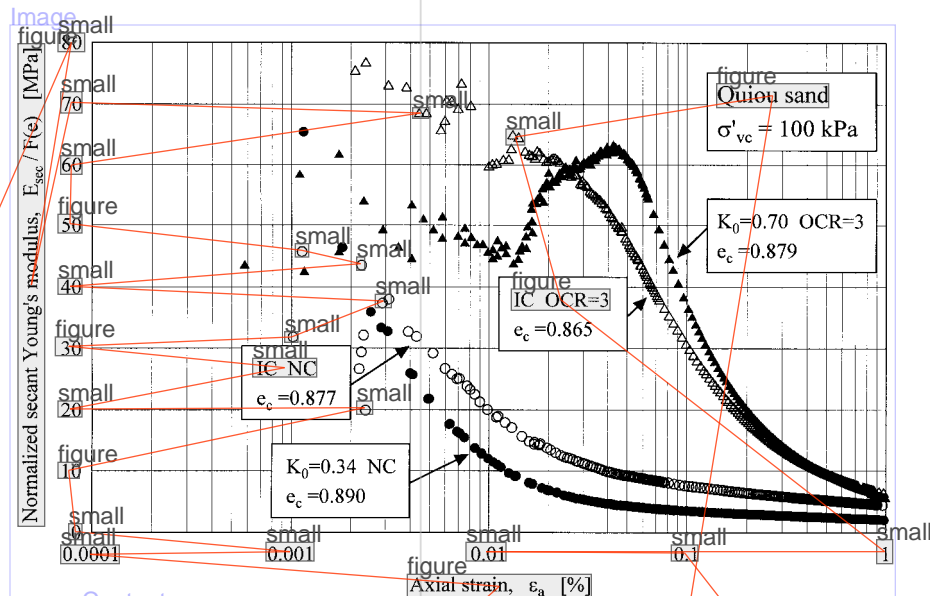


FIG. 2. Secant Young's Modulus versus Axial Strain of Quiou Sand

tion stress (100 kPa) but subject to different consolidation stress ratios ( $K_c = 1$  and  $K_c = K_0$ ) and histories ( $1 \leq \text{OCR} \leq 3$ ). In order to eliminate the effect of the difference of density on test results in these figures, the secant Young's modulus was normalized by dividing it by the following void ratio functions: Toyoura sand  $F(e) = (2.17 - e)^2/(1 + e)$  (Iwasaki et al. 1978), while for Quiou sand  $F(e) = (3.82 - e)^2/(1 + e)$  (Fioravante et al. 1994a).

In spite of a certain scatter observed at very small strain ( $\epsilon_a \leq 5 \times 10^{-5}$ ), it can be seen that the small strain secant Young's modulus  $E_0$  of Toyoura sand is virtually the same for the four tests [ $E_0/F(e) \approx 250$  MPa], that is, it does not depend on the  $K_c$ , the horizontal stress  $\sigma'_h$ , or the OCR, being only a function of the axial consolidation stress. On the other hand, in the case of Quiou sand, the small strain secant Young's modulus of the OC specimens [ $E_0/F(e) \approx 60$  to 70 MPa] is higher than that of the NC specimens [ $E_0/F(e) \approx 40$  to 50 MPa]. In other words, for a clean sand, such as Toyoura sand, the  $E_0$  value is a function of the effective axial stress and is quite independent of the radial effective stress and the stress history, as already shown by Flora et al. (1994), Kohata et al. (1994), and Lo Presti et al. (1995). In the case of sand containing crushable material, such as Quiou sand, although  $E_0$  does not depend on the  $K_c$  or the  $\sigma'_h$ , it instead depends on the stress history (Lo Presti et al. 1995).

On the other hand, at intermediate strain, it can be seen that the reduction of  $E_{\text{sec}}$  in NC specimens occurs for  $\epsilon_a$  larger than 0.001%. It can be also seen that the reduction of  $E_{\text{sec}}$  in NC Quiou sand is much more pronounced than that observed for NC Toyoura sand; for example,  $E_{\text{sec}}/E_0$  at  $\epsilon_a = 0.01\%$  is about 0.55 in the NC Toyoura specimen and is about 0.45 in the NC Quiou specimen. In the case of OC specimens, the sudden reduction of  $E_{\text{sec}}$  occurs for strain levels larger than about 0.05% for both sands. This experimental fact indicates that the amount of plastic deformation decreased for axial strain by as much as 0.05%, as a consequence of the mechanical overconsolidation. It is said that the linear threshold strain increases according to the overconsolidation history, as reported by Jardine et al. (1984) and Tatsuoka and Kohata (1994).

## STIFFNESS NONLINEARITY

### Empirical Fitting Equation

In order to evaluate the effects of the confining pressure, the stress ratio at consolidation, and the overconsolidation his-

tory on the secant Young's modulus  $E_{\text{sec}}$  under small and intermediate strain levels, an empirical study was performed on a large number of triaxial compression test results on Toyoura, Quiou, and Ticino sands.

It has generally been recognized that the shear modulus of sand can be expressed by means of an empirical equation as a function of the void ratio, the confining pressure, and strain levels (Hardin and Richart 1963; Iwasaki and Tatsuoka 1977; Jamiolkowski et al. 1994a). For example, Iwasaki and Tatsuoka indicated that the shear modulus of clean sands obtained from resonant column and cyclic torsional tests can be expressed by

$$G_{eq} = K(\gamma)F(e)p'^{n(\gamma)} \quad (1)$$

where  $G_{eq}$  = equivalent shear modulus;  $K(\gamma)$  = material constant that depends on shear strain level;  $F(e)$  = void ratio function;  $p'$  = mean effective stress; and  $n(\gamma)$  = empirical exponent that depends on shear strain level.

According to Hardin and Blandford (1989), it is also possible to express the dependence of the small strain shear modulus  $G_0$  on the current state of a soil by means of the following relationship:

$$G_0 = S_{ij}F(e)(\text{OCR})^k p_a^{(1-n_i-n_j)} \sigma_i'^{n_i} \sigma_j'^{n_j} \quad (2)$$

where  $S_{ij}$  = nondimensional material constant of given soil that also reflects its fabric;  $k$  = empirical exponent that depends on plasticity index ( $PI$ ) of soil;  $\sigma_i'$  and  $\sigma_j'$  = effective principal stresses acting on plane in which  $G_0$  is measured;  $n_i$  and  $n_j$  = empirical exponents; and  $p_a$  = reference stress.

Moreover, Hardin and Blandford suggested that the Young's modulus for elastic compressive strain increments in a certain direction is a unique function of the normal stress in that direction. Lo Presti et al. (1995) and Hoque and Tatsuoka (1998) reported similar results for triaxial tests performed on clay and sand.

As mentioned before, it was indicated that the secant Young's modulus depends on the stress ratio and the stress history under consolidation. Moreover its effects were different from sand to sand. Thus, to clarify the effects of the confining pressure, the stress ratio at consolidation (i.e., isotropic and  $K_0$  consolidation) and the overconsolidation history on the secant Young's modulus  $E_{\text{sec}}$  under wide strain levels (0.001 to 1%), an empirical study was performed on triaxial compression test results using the following equations:



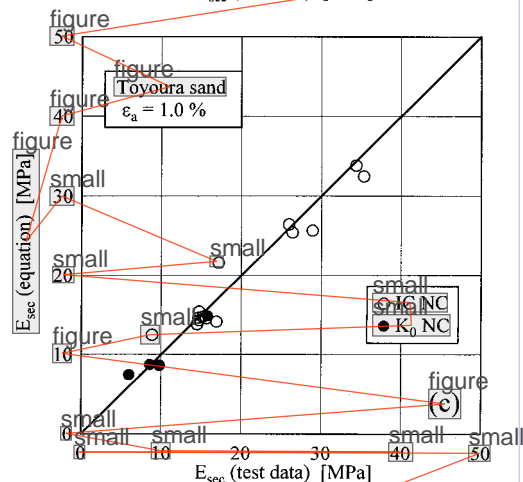
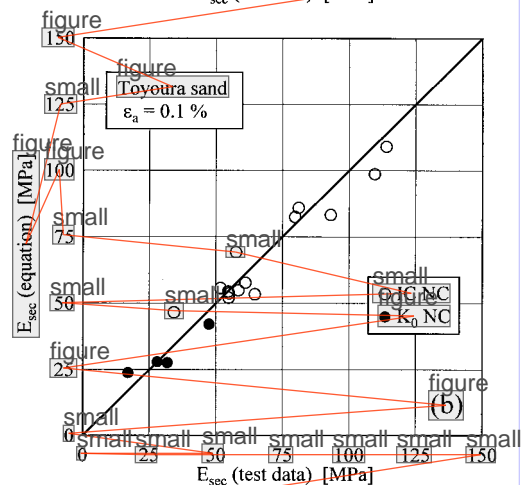
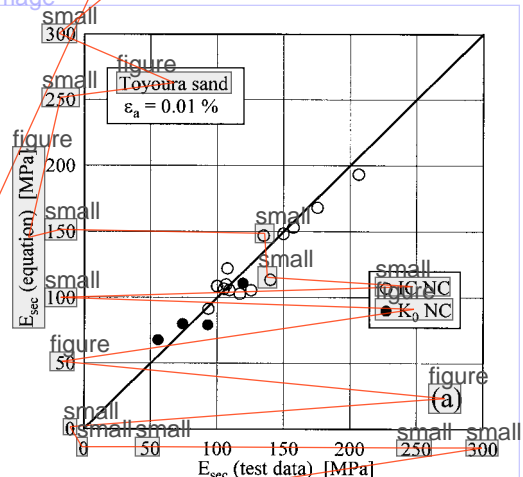
$$E_{\text{sec(IC)}} = S_v F(e) \sigma'_w p_a^{(1-n)} \quad (\text{isotropic normally consolidated sand}) \quad (3)$$

Math - Large Block

$$E_{\text{sec}(K_0)} = a S_v F(e) \sigma'_w p_a^{(1-n)} \quad (K_0 \text{ normally consolidated sand}) \quad (4)$$

where  $S_v$  = nondimensional material constant that depends on axial strain level of isotropic normally consolidated sands;  $F(e)$  = void ratio function [ $F(e) = (2.17 + e)^2 / (1 + e)$  (Toyoura and Ticino sands) and  $F(e) = (3.82 - e)^2 / (1 + e)$  (Quiou sand)];  $\sigma'_w$  = effective axial stress at end of consolidation;  $n$  = empirical exponent that depends on axial stress and axial strain level of isotropic normally consolidated sands;  $p_a$  = reference stress (98 kPa); and  $a$  = empirical constant that

Image

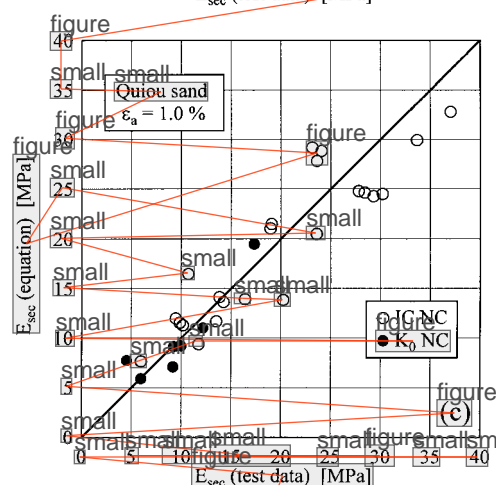
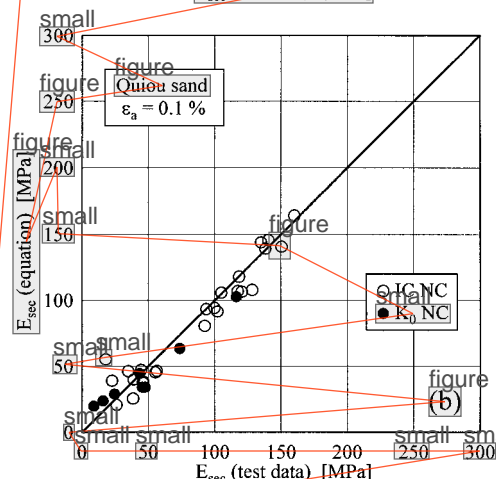
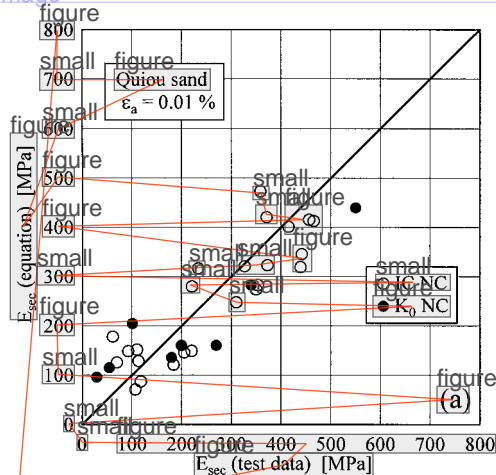


ImageDescription

**FIG. 3. Comparison of Empirical Fitting Study and Test Data on Toyoura Sand: (a)  $\epsilon_a = 0.01\%$ ; (b)  $\epsilon_a = 0.1\%$ ; (c)  $\epsilon_a = 1.0\%$**

headerOrFooter

Image



ImageDescription

**FIG. 4. Comparison of Empirical Fitting Study and Test Data on Quiou Sand: (a)  $\epsilon_a = 0.01\%$ ; (b)  $\epsilon_a = 0.1\%$ ; (c)  $\epsilon_a = 1.0\%$**

Content

depends on axial strain level of  $K_0$  normally consolidated sands.

Figs. 3–5 show the comparison of the secant modulus obtained from the test data and the empirical fitting equation for normally consolidated [isotropic consolidated (IC) and  $K_0$  consolidated ( $K_0$ C)] Toyoura, Quiou, and Ticino sands for three kinds of strain levels, respectively. Although a certain scatter is recognized, it can be seen that the empirical fitting equation that uses (3) and (4) above agrees well with the test data at small and intermediate strain levels and stress ratios for normally consolidated sands. Table 3 lists the parameter values of the empirical fitting equation for the three sands.

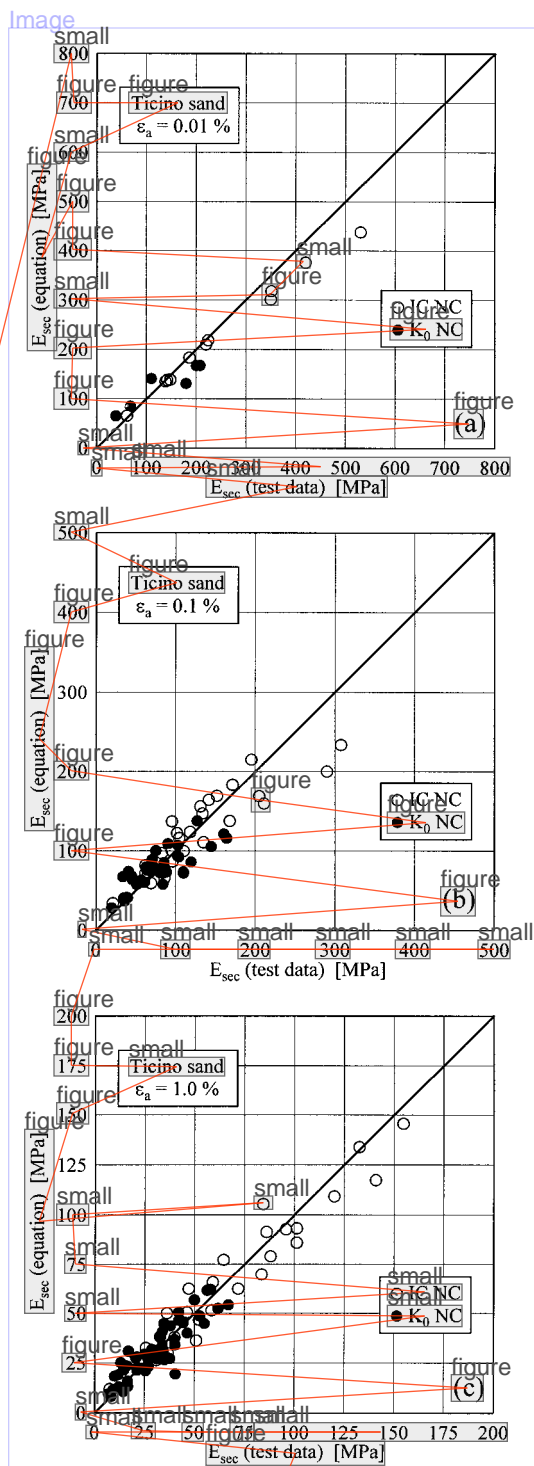


**FIG. 5. Comparison of Empirical Fitting Study and Test Data on Ticino Sand: (a)  $\varepsilon_a = 0.01\%$ ; (b)  $\varepsilon_a = 0.1\%$ ; (c)  $\varepsilon_a = 1.0\%$**

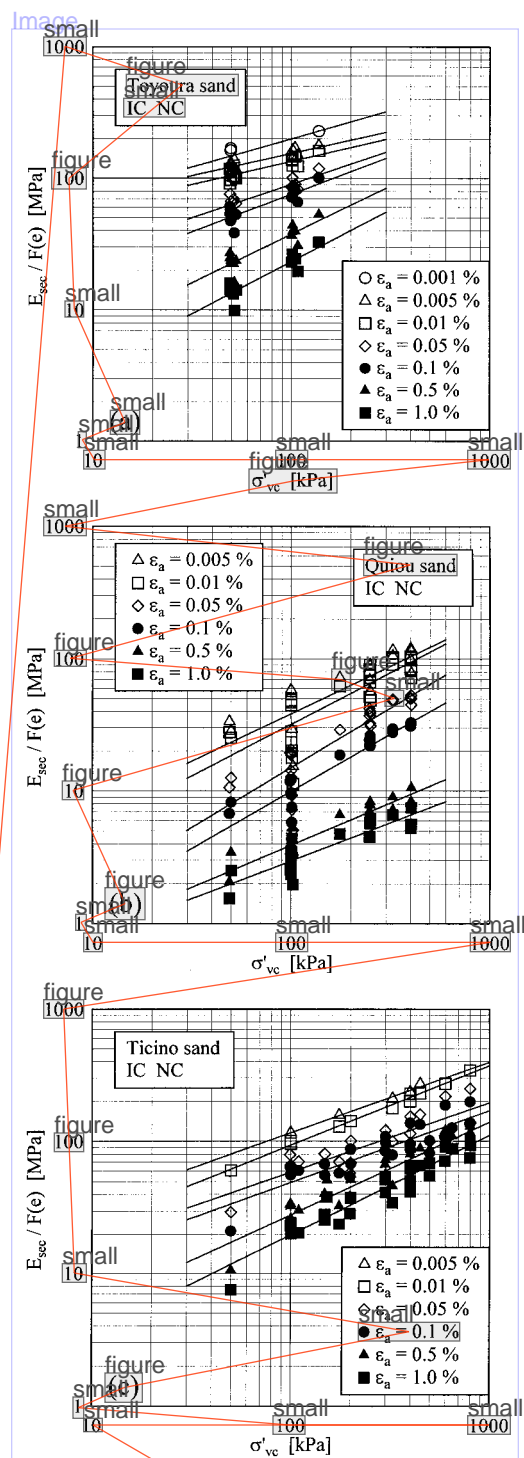


**FIG. 6. Normalized Secant Young's Modulus versus Effective Vertical Stress at Consolidation: (a) Toyoura Sand; (b) Quiou Sand; (c) Ticino Sand**

### Influence Factors

### Consolidation Stress

Fig. 6 shows the variations of  $E_{sec}/F(e)$  at several strain levels with respect to effective axial stress  $\sigma'_{vc}$  using double logarithmic scales for isotropic NC Toyoura, Quiou, and Ticino sand specimens. From this figure, it has been found that the relationships between  $\log(E_{sec}/F(e))$  and  $\log(\sigma'_{vc})$  for each strain level and sand can be approximated as a straight line. Accordingly, the secant Young's modulus of isotropic NC sand specimens can be explained by an exponent function of the

effective vertical stress at any strain level, as in the case of small strains.

Fig. 7 shows the relationships of  $n$ -value versus  $\log(\varepsilon_a)$  for Toyoura, Quiou, and Ticino sand specimens. The strain level dependency of the  $n$ -value of Toyoura sand is similar to that of Ticino sand. The  $n$ -values at small strain levels of Toyoura and Ticino sands are almost equal to 0.5, and those increase gradually with the increase in the strain levels. On the other hand, in the case of Quiou sand, the  $n$ -value increases at lower strain levels than other sands, and for  $\varepsilon_a > 0.05\%$  it decreases with an increase in the strain levels. It would seem that this is the effect of the high crushability of Quiou sand. Fig. 8

Image

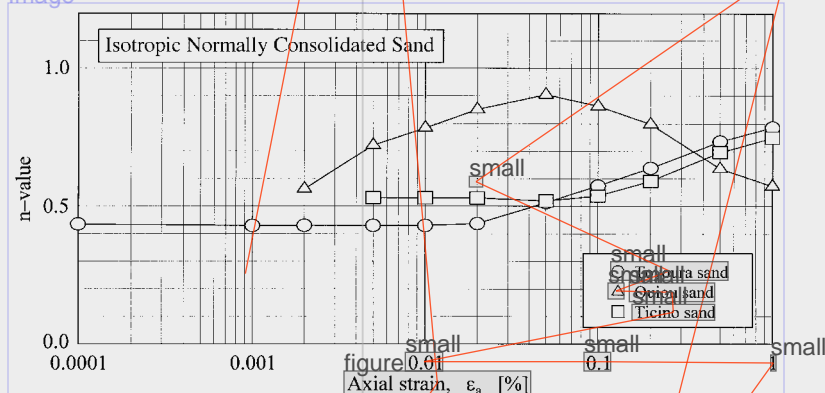
figure

**TABLE 3. Parameter Values of Empirical Fitting Equation**

Toyoura Sand				Quiou Sand			Ticino Sand		
figure (1)	figure (2)	figure (3)	a (for $K_0$ ) (4)	n (5)	$S_v$ (6)	a (for $K_0$ ) (7)	figure (8)	figure (9)	figure a (for $K_0$ ) (10)
0.0001	0.434	2,122	1.04	—	—	—	—	—	—
0.001	0.430	2,028	1.01	—	—	—	—	—	—
0.002	0.430	1,666	1.08	0.562	512	0.83	—	—	—
0.005	0.430	1,572	0.78	0.722	387	0.66	0.531	1,173	small
0.01	0.430	1,367	0.56	0.785	321	0.76	0.530	946	small
0.02	0.437	1,122	0.46	0.852	246	0.70	0.530	742	small
0.05	0.513	911	0.38	0.905	150	0.58	0.519	585	small
0.1	0.524	763	0.35	0.864	99.6	0.50	0.538	497	small
0.2	0.628	599	0.34	0.799	64.2	0.47	0.591	418	small
0.5	0.736	378	0.34	0.636	39.3	0.51	0.690	282	small
1	0.786	234	0.35	0.573	30.0	0.51	0.749	199	small

Note:  $E_{sec(IC)} = S_v F(e) \sigma_{v-c}^{m(1-n)/a}$  (isotropic normally consolidated);  $E_{sec(K_0)} = a E_{sec(IC)}$  ( $K_0$  normally consolidated);  $F(e) = (2.17 - e)^2 / (1 + e)$  (Toyoura and Ticino sands); and  $F(e) = (3.82 - e)^2 / (1 + e)$  (Quiou sand).

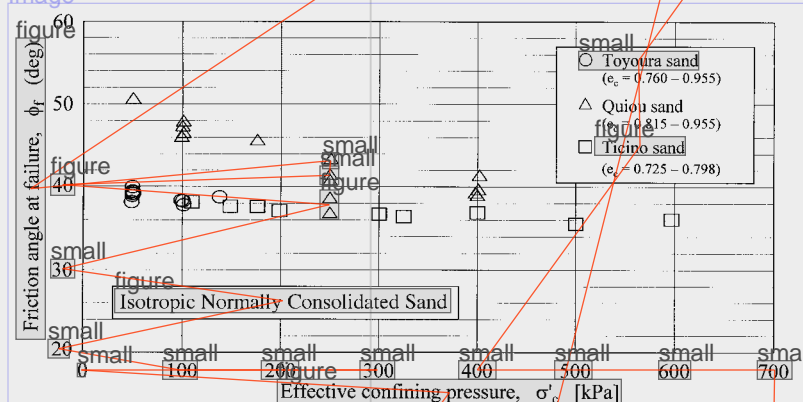
Image



ImageDescription

**FIG. 7. Effect of Strain level on  $n$ -Value**

Image



ImageDescription

**FIG. 8. Stress Dependency of Friction Angle at Failure**

Content

shows the stress dependency of the friction angle at failure for isotropic NC specimens. It has been found that the stress dependency of Quiou sand is larger than that of Toyoura and Ticino sands. In particular, the friction angle of Quiou sand decreases rapidly with an increase in the confining pressure. This is because the crushability of Quiou sand is higher than that of other sands. Therefore, the  $n$ -value of Quiou sand decreased for  $\epsilon_a > 0.05\%$ .

Headline

**Consolidation Stress Ratio**

The secant modulus decrease with an increase in the strain level is more pronounced in  $K_0$  consolidated ( $K_0C$ ) specimens than in isotropic consolidated (IC) specimens, as mentioned before.

headerOrFooter

headerOrFooter

Content

Fig. 9 shows the relations of the material constant  $S_v \times F(e)$  (for IC) or  $a \times S_v \times F(e)$  (for  $K_0C$ ) versus  $\log(\epsilon_a)$  to better clarify the effect of the strain level on the secant modulus. It can be seen that the reductions of material constants predominantly occur for strain levels that are larger than about 0.001%. The reduction of material constant of IC Quiou sand is larger than those of Toyoura and Ticino sands. In addition, the reduction of the material constants of  $K_0C$  specimens is larger than that of IC specimens.

Fig. 10 shows the relationships between the ratio of the secant Young's modulus  $E_{sec(K_0)}/E_{sec(IC)}$  (i.e.,  $a$ -value) and  $\log(\epsilon_a)$  for NC specimens. It has been found that the  $E_{sec(K_0)}/E_{sec(IC)}$  at small strains are nearly equal to one. It has also been found that the  $E_{sec(K_0)}/E_{sec(IC)}$  decreases with an increase in the strain level.

Downloaded from ascelibrary.org by Massachusetts Institute of Technology (MIT) on 05/23/23. Copyright ASCE. For personal use only; all rights reserved.

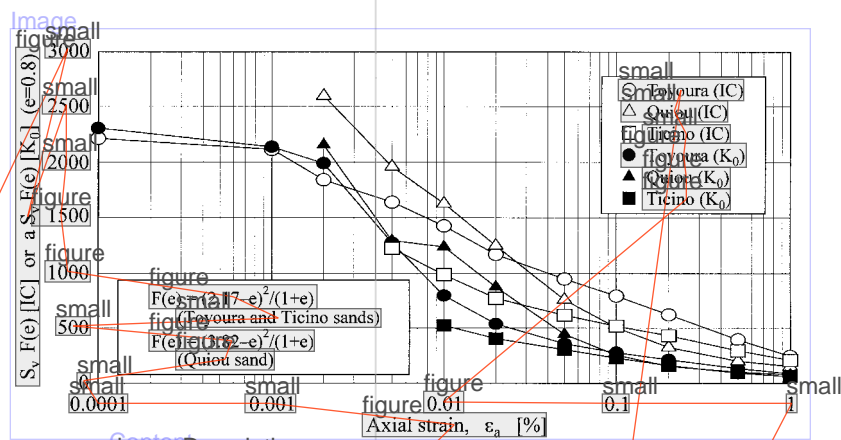


FIG. 9. Strain Level Dependency of Material Constant

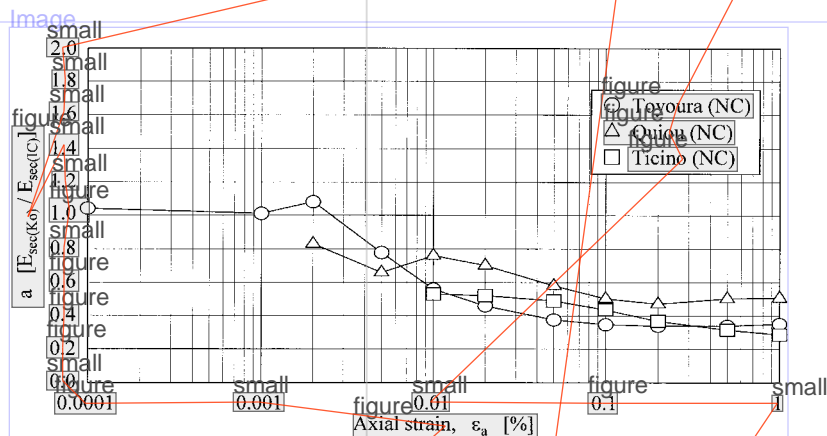


FIG. 10. Effect of Consolidation Stress Ratio

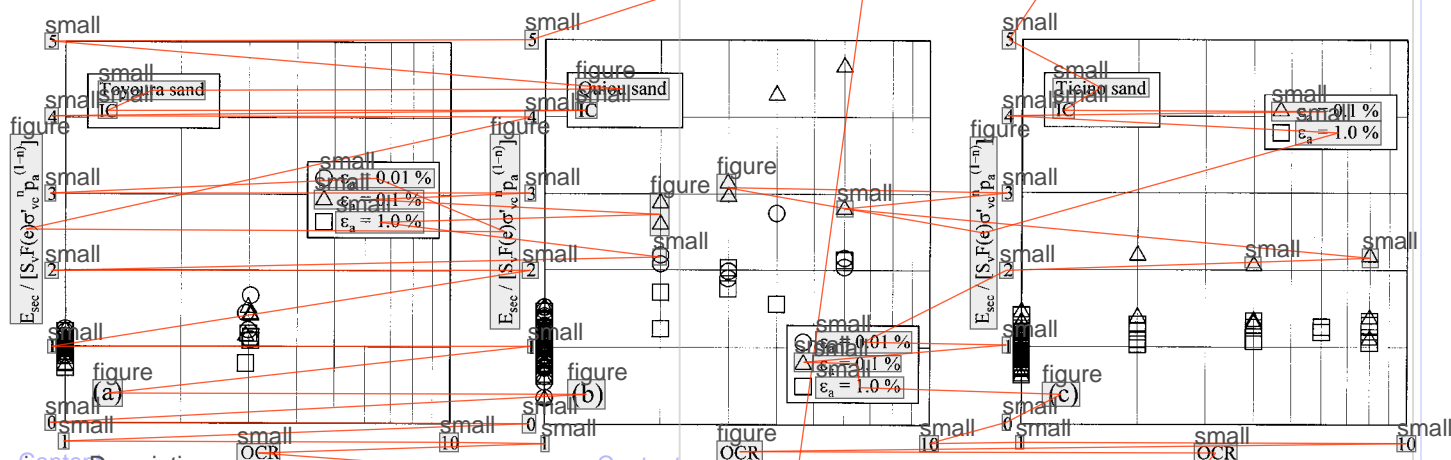


FIG. 11. Normalized Secant Young's Modulus versus Overconsolidation Ratio: (a) Toyoura Sand; (b) Quiou Sand; (c) Ticino Sand

#### Overconsolidation Ratio (OCR)

It has been shown that the secant Young's modulus was significantly dependent on overconsolidation history. Fig. 11 shows the variations of normalized secant Young's modulus  $E_{sec} / [S_v F(e) \sigma_{vc}^{(1-n)}]$ , with respect to OCR, as examined using a single logarithmic scale at several strain levels for IC Toyoura, Quiou and Ticino sand specimens. From this figure, it has been found that the effects of overconsolidation history on the secant Young's modulus for Quiou sand are larger than those for Toyoura and Ticino sands.

Figs. 12(a-c) show the typical relations of the secant modulus normalized by void ratio function and confining pressure versus  $\log(\epsilon_a)$  to better clarify the effect of the overconsolidation on the secant modulus for the three IC and  $K_0$ C sand specimens, respectively. In these figures, the normalized secant

modulus for isotropic and  $K_0$  normally consolidated specimens were indicated by the  $S_v$ -value or  $a \times S_v$ -value in (3) and (4), respectively. Fig. 13 shows the variation of the  $K_0$ -value after consolidation, due to the difference in the overconsolidation ratio.

It can be seen that the strain level at which the reduction of  $E_{sec}$  in OC specimens occurs is larger than that in NC specimens. It can be also seen that the sudden reduction of  $E_{sec}$  in OC specimens that occurs for  $\epsilon_a$  is larger than about 0.05% for all sands. In addition, it is found that the reduction tendency of  $E_{sec}$  is relatively similar for isotropic and  $K_0$  OC specimens for the same OCR. This is because (1) the yield locus (the linear threshold strain) expanded because of the overconsolidation history; and (2) the  $K_0$ -value of the OC specimen increases with an increase in the overconsolidation ratio, as shown in Fig. 13.



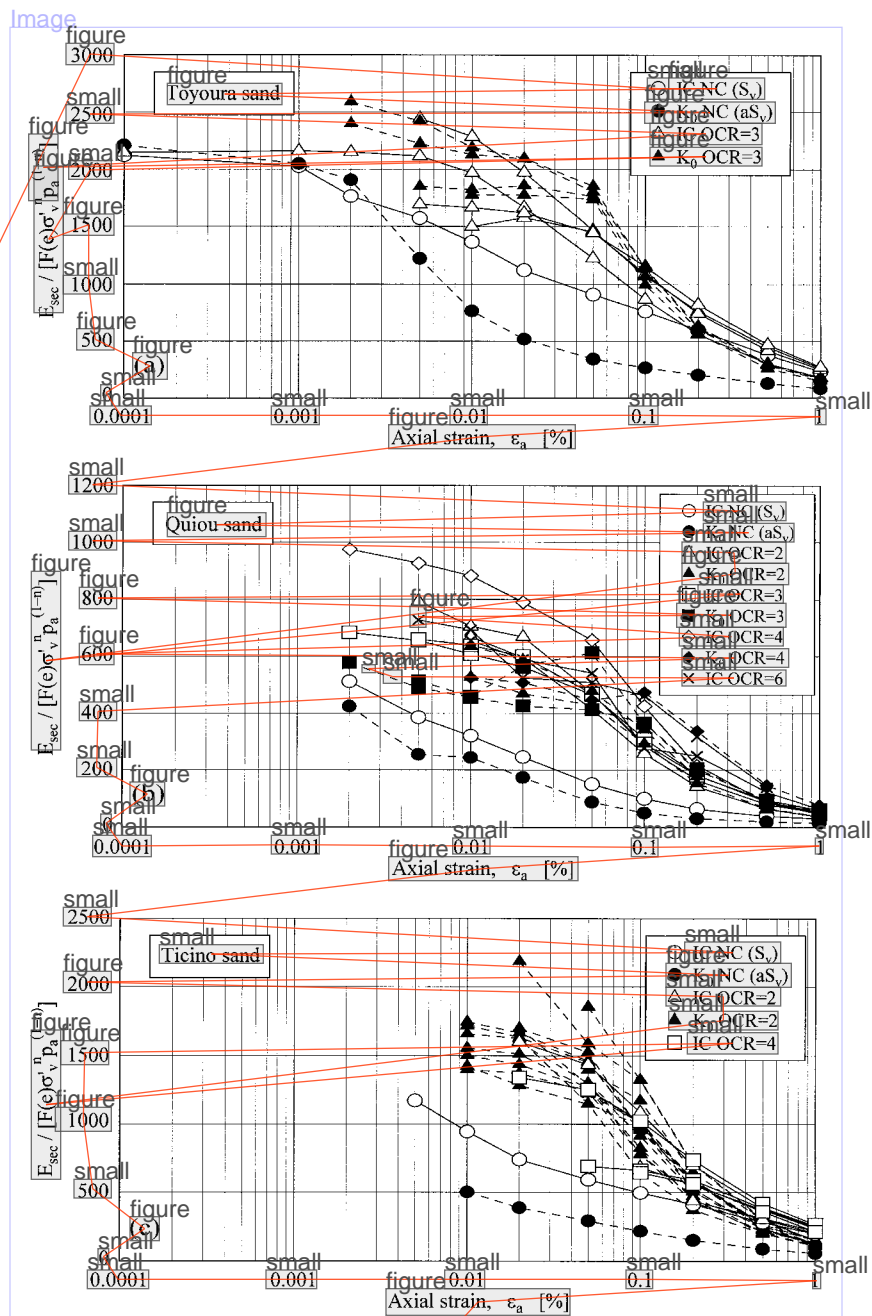


FIG. 12. Typical Relations of Normalized Secant Young's Modulus versus Axial Strain: (a) Toyoura Sand; (b) Quiou Sand; (c) Ticino Sand

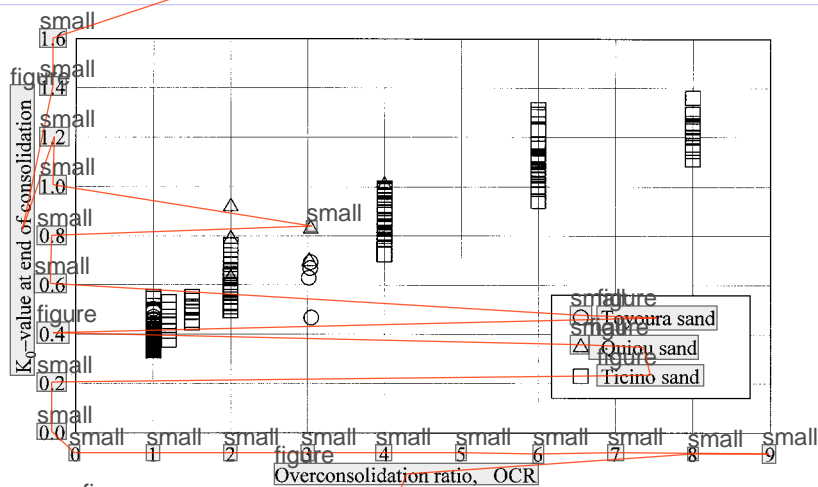


FIG. 13. Effect of Overconsolidation History on  $K_0$ -Value



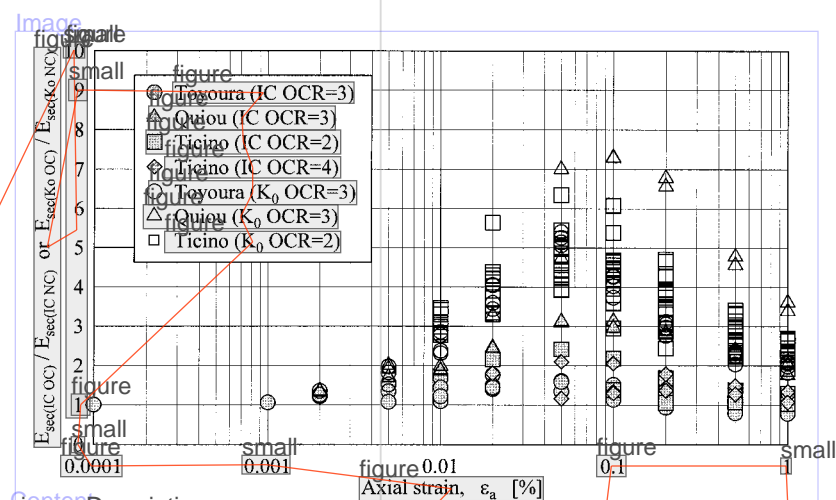


FIG. 14. Effect of Overconsolidation History on Secant Young's Modulus

Fig. 14 shows the relationships of the secant modulus ratios  $E_{\text{sec}}(\text{OC})/E_{\text{sec}}(\text{NC})$  versus  $\log(\epsilon_a)$  for isotropic and  $K_0$  consolidated Toyoura (OCR = 3), Quiou (OCR = 3), and Ticino (OCR = 2, 4) sand specimens. It has been found that the effects of the overconsolidation history for Toyoura sand are negligibly small at small strain levels. The effects of the OC history on the secant modulus are greatest at  $\epsilon_a$ , around 0.05 to 0.1%. The effects of the OC history are similar on Toyoura and Ticino sands. On the other hand, the effects of OC history on Quiou sand are much larger than for other sands. This can be seen because the soil particle crush of Quiou sand had significantly progressed because of the OC history and shearing.

It has also been found that the effects of OC history on  $K_0$ C specimens are larger than those on IC specimens. This is because (1) the secant Young's modulus of  $K_0$  specimens is smaller than that of the IC specimen, except that at small strain levels under the same vertical consolidation stress, as shown in Fig. 12, and (2) the  $K_0$ -value increases with an increase in OCR, as shown in Fig. 13. Consequently, the effects of OC history on the secant Young's modulus of the  $K_0$ C specimen were larger than those of the IC specimens.

## CONCLUSIONS

This paper presents the analysis of a large number of drained triaxial compression tests, many of which were carried out with local strain measurement. The tests were performed on both isotropically and anisotropically consolidated specimens of three sands prepared by pluvial deposition in air and allow the following conclusions, all of which refer to the value of sand moduli at  $\sigma'_v = 100$  kPa:

1. For all three sands, the secant Young's modulus normalized with respect to the consolidation void ratio exhibits very pronounced degradation with increasing strain.
2. Nonlinearity starts to show when the axial strain exceeds  $\approx 1 \times 10^{-3}$  and  $5 \times 10^{-2}\%$  for NC and OC with OCR = 3 specimens, respectively.
3. Below such a strain level, which corresponds to the linear threshold strain, the secant Young's modulus coincides with the initial tangent stiffness ( $E_0$ ), which depends only on the magnitude of  $\sigma'_v$ , being independent of  $\sigma'_h$ .
4. For silica Ticino and Toyoura sands, the  $E_0$  results were found to be independent of OCR, while in carbonatic Quiou sands it moderately influences the magnitude of the initial stiffness.
5. Beyond the linear threshold strain, the reduction of  $E_{\text{sec}}$  for normally consolidated specimens can be matched by the empirical fitting formulae.

6. For isotropically consolidated specimens, the stress exponent  $n$  of  $\sigma'_v$  increases gradually from a minimum value (0.43 to 0.56) at very small  $\epsilon_a$  with the increase in the strain levels. In this respect, the irregular trend of  $n$  versus  $\epsilon_a$ , observed for Quiou sand, cannot be explained. However, it could be due to the pronounced grains' crushability.

7. The effect of overconsolidation on the secant modulus was found to be highly axial strain level dependent. As has been shown by many researchers, it is insignificant for silica sands at very small strain ( $\epsilon_a = 1 \times 10^{-3}\%$ ), increasing thereafter with an increase of the strain and reaching the maximum values at  $\epsilon_a$  around 0.05 to 0.1%. The influence of OCR on the  $E_{\text{sec}}$  results are more pronounced for the anisotropically  $K_0$ -consolidated specimens than for those subjected to isotropical consolidation.

Overall, the phenomenological examination of the drained triaxial compression tests results gathered for three sands has shown that, in the strain range of 0.01 to 0.1%, the soil stiffness under axisymmetric loading conditions exhibits a highly pronounced nonlinearity and is strongly influenced by the test conditions, in particular, the consolidation stress ratio and OCR.

The data presented here provide evidence of the inadequacy of some existing quasilinear fitting equations (e.g., conventional hyperbola) to reproduce the variation of  $E_{\text{sec}}$  in the strain range of practical interest. Moreover, data presented in this paper can guide practitioners in selecting the equivalent stiffness that can be used for simple calculations using the formula of the theory of elasticity.

## APPENDIX. REFERENCES

- references
- Belotti, R., Jamiolkowski, M., Lo Presti, D. C. F., and O'Neill, D. A. (1996). "Anisotropy of small strain stiffness in Ticino sand." *Geotechnique*, London, 46(1), 115–131.
- Fioravante, V., Capoferri, R., Hameury, O., and Jamiolkowski, M. (1994a). "Deformation characteristics of uncemented carbonate Quiou sand." *Pre-failure deformation of geomaterials*, S. Shibuya, T. Mitachi, and S. Miura, eds., Balkema, Rotterdam, The Netherlands, 1, 55–61.
- Fioravante, V., Jamiolkowski, M., and Lo Presti, D. C. F. (1994b). "Stiffness of carbonatic Quiou sand." *Proc., 13th Int. Conf. on Soil Mech. and Found. Engrg.*, New Delhi, 163–167.
- Flora, A., Jiang, G. L., Kohata, T., and Tatsuoka, F. (1994). "Small strain behavior of a gravel along some triaxial stress paths." *Pre-failure deformation of geomaterials*, S. Shibuya, T. Mitachi, and S. Miura, eds., Balkema, Rotterdam, The Netherlands, 1, 279–285.
- Hardin, B. O., and Bladford, G. E. (1989). "Elasticity of particulate materials." *Geotech. Engrg., ASCE*, 115(6), 788–805.
- Hardin, B. O., and Richart, F. E. (1963). "Elastic wave velocities in granular soils." *J. Soil Mech. and Found. Div., ASCE*, 89(1), 33–65.

Downloaded from ascelibrary.org by Massachusetts Institute of Technology (MIT) on 05/23/23. Copyright ASCE. For personal use only; all rights reserved.

References

references

Hoque, E., and Tatsuoka, F. (1998). "Anisotropy in elastic deformation of granular materials." *Soils and Found.*, Tokyo, 38(1), 163–179.

Iwasaki, T., and Tatsuoka, F. (1977). "Effects of grain size and grading on dynamic shear moduli of sands." *Soils and Found.*, Tokyo, 17(3), 19–25.

Iwasaki, T., Tatsuoka, F., and Takagi, Y. (1978). "Shear moduli of sands under cyclic torsional shear loading." *Soils and Found.*, Tokyo, 18(1), 69–76.

Jamiolkowski, M., Lancellotta, R., and Lo Presti, D. C. F. (1994a). "Remarks on stiffness at small strains of six Italian clays." *Pre-failure deformation of geomaterials*, S. Shibuya, T. Mitachi, and S. Miura, eds., Balkema, Rotterdam, The Netherlands, 2, 817–836.

Jamiolkowski, M., Lancellotta, R., Lo Presti, D. C. F., and Pallara, O. (1994b). "Stiffness of Toyoura sand at small and intermediate strain." *Proc., 13th Int. Conf. on Soil Mech. and Found. Engrg.*, New Delhi, 169–173.

Jardine, R. J., Symes, M. J., and Burland, J. B. (1984). "The measurement of soil stiffness in the triaxial apparatus." *Géotechnique*, London, 34(3), 323–340.

References

references

Kohata, Y., Tatsuoka, F., Dong, J., Teachavorasinskun, S., and Mizumoto, K. (1994). "Stress-state affecting elastic deformation moduli of geomaterials." *Pre-failure deformation of geomaterials*, S. Shibuya, T. Mitachi, and S. Miura, eds., Balkema, Rotterdam, The Netherlands, 1, 3–9.

Lo Presti, D. C. F., Jamiolkowski, M., Pallara, O., Pisciotta, V., and Ture, S. (1995). "Stress dependence of sand stiffness." *Proc., 3rd Int. Conf. on Recent Adv. in Geotech. Earthquake Engr. and Soil Dyn.*, University of Missouri, Rolla, 71–76.

Lo Presti, D. C. F., Pallara, O., Raino, M., and Maniscalco, R. (1994). "A computer-controlled triaxial apparatus: Preliminary results." *Italian Geotech. Rev.*, Rome, 28(1), 43–60.

Tatsuoka, F. (1988). "Some recent developments in triaxial testing system for cohesionless soils." *Advanced triaxial testing of soil and rock, ASTM STP 977*, 7–67.

Tatsuoka, F., and Kohata, Y. (1994). "Stiffness of hard soils and soft rocks in engineering applications." *Pre-failure deformation of geomaterials*, S. Shibuya, T. Mitachi, and S. Miura, eds., Balkema, Rotterdam, The Netherlands, 2, 947–1063.